

User-Adaptive Inertial Sensor Network for Feedback-Controlled Gait Support Systems

David Graurock, Thomas Schauer, Thomas Seel

Abstract—Inertial sensor networks on the lower limbs enable realtime assessment of gait and thus feedback control of active gait support systems. However, most state-of-the-art methods (1) require each sensor unit to be attached to a predefined segment in a predefined orientation, or (2) require the user to perform precise calibration motions, and (3) require a homogeneous magnetic field. Such requirements are incompatible with most clinical applications especially if the patient attaches the sensor autonomously. We propose methods for a plug-and-play gait analysis that uses only accelerometer and gyroscope readings. These methods allow the sensor network to adjust to the user and to calibrate itself automatically using data from only five seconds of walking, i.e. the methods are *plug-and-play*. In particular, we present a *sensor-to-segment pairing* method that identifies which sensor is attached to which body segment (thigh, shank and foot) of which leg. Analysis of data from over 500 trials with healthy subjects and Parkinson’s patients yields a correct-pairing success rate of 99.8%. Additionally, we present a *sensor-to-segment calibration* method that determines the knee joint axis in the local coordinates of each sensor, which is essential for joint angle calculation. Comparing the resulting knee joint angles to measurements of an optical motion capture system yields root-mean-square deviations of about 3° .

I. INTRODUCTION

Active exoskeletons, FES neuroprostheses and biofeedback systems can support patients with walking disabilities and help them to regain individual mobility, see for example [1]–[3]. All of these assistive technologies require realtime assessment of the patient’s gait. State-of-the-art inertial sensors (inertial measurement units, IMUs) can provide accurate measurements while overcoming the restrictions of conventional (i.e. optoelectronic) motion analysis. IMUs have become so small and lightweight that they are easily integrated into textiles or worn on the skin.

However, inertial motion analysis is still too restrictive with regard to its usability in many clinical applications. Each IMU must be attached to a predefined body segment, and precisely defined calibration movements must be performed (see for example [4] and [5]). As Cereatti et. al. [6] recently pointed out, the common calibration procedures are hardly applicable in daily life. Therefore, sensor-to-segment pairing and calibration represent major challenges in IMU-based gait analysis.

Some recent contributions have demonstrated that sensor-to-segment calibration can be achieved without the need for precise calibration movements, see for example [7], [8]. However, prior knowledge is required about which sensor is attached to which body segment. Especially in clinical applications, the reliability of inertial gait analysis should not depend on the user attaching each IMU correctly to its designated body segment. A number of studies have aimed to overcome this restriction by proposing methods for on-body localization of IMUs, for example [9]–[12]. These methods

result in accuracies of up to 100%. However, they are either based on learning algorithms that process large offline data sets or they require the user to perform predefined motions.

In the present contribution, we consider IMUs on the lower limbs and present a computationally low-cost method that identifies to which segments the sensors are attached. The method exploits characteristic features of the inertial data that is measured during gait, i.e. it does *not* require the user to perform any static pose. In addition, we briefly present a method that identifies the sensor-to-segment orientation while the subject walks. The combination of both methods yields a plug-and-play solution for sensor-to-segment pairing and calibration of inertial sensor networks during gait (see Figure 1).

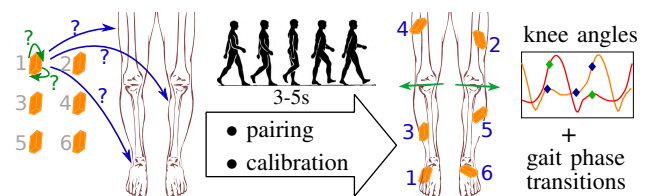


Figure 1: Plug-and-play sensor-to-segment pairing and calibration: After a few steps, the algorithms determine which sensor is attached to which leg segment and in which orientation it is attached. Based on this information, knee joint angles and gait phases can be determined in realtime.

II. USER-ADAPTIVE REALTIME GAIT ANALYSIS

Throughout this contribution, we consider a setup of one IMU on the *thigh*, *shank* and on the *foot* for both legs. Each IMU provides 3D accelerometer readings as well as 3D gyroscope readings at a measurement sample rate of $f_s = 50$ Hz. We assume that it is unknown which sensor is attached to which body segment (*thigh*, *shank* and *foot*) and in which orientation the sensors are attached to the segments. Instead, this information will be automatically determined from the data measured during walking.

A. Sensor-to-Segment pairing

We aim to develop an easy-to-implement and computationally low-cost method that processes the realtime measurement data of an inertial sensor network to find out which sensor is attached to which body segment (thighs, shanks, and feet of both legs). Since we have no prior knowledge about the sensor-to-segment orientations, the method should only use the Euclidean norms of the measured three-dimensional accelerations and angular rates. To minimize the influence of signal fluctuation, we always apply sufficient low-pass filtering to these measurement signals. Furthermore, we want to use only relative comparisons of characteristic signal values, since absolute values and thresholds typically change with gait velocity as well as from subject to subject.

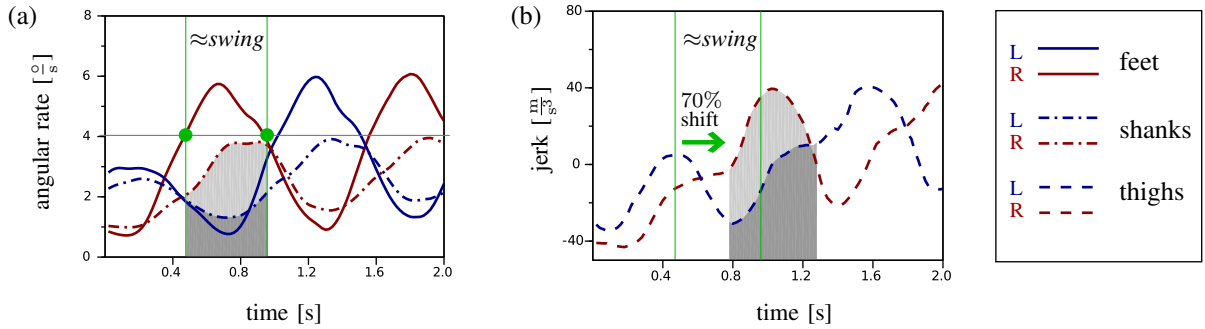


Figure 2: (a) Low-pass-filtered angular rates for one foot sensor and both shank sensors. Green dots indicate when the angular rate of the foot rises/falls above/below the all-time maximum angular rate (horizontal line) of both shank sensors. These events define the beginning and the end of the approximate swing phase (vertical lines). Integrating the signals over this time interval allows evaluation of Feature 3. (b) Low-pass-filtered zero-mean jerk of both thigh sensors. The integration interval that is used for evaluation of Feature 4 is shifted by 70% of $T_{\approx swing}$ as indicated by the green arrow.

In order to find robust criteria for sensor-to-segment pairing, we analyzed a large number of characteristics and features in the signals recorded during gait. For the sake of brevity, we only present the most useful and robust features in the present contribution. The proposed sensor-to-segment pairing algorithm consists of four consecutive steps:

- Identification of the *foot* sensors
- Identification of the *shank* and *thigh* sensors
- Pairing of the *shank* sensors to their related *foot* sensors
- Pairing of the *thigh* sensors to their related *foot* sensors

Each of these identification steps is based on a few seconds of data recorded during walking. For the first step, i.e. finding out which sensors are attached to the feet, we propose the following simple criterion:

Feature 1: *Foot sensors have the highest all-time maximum of low-pass-filtered acceleration.*

Here and in the following we use the term *all-time* to emphasize that this maximum is determined (for each sensor) over the entire period of time that is analyzed.

Once the *foot* sensors are identified, other methods can be employed to obtain realtime information on the current gait phase and orientation of both feet (see for example [13] or [15] and [14]). We continue the sensor-to-segment pairing by distinguishing between the *thigh* and *shank* sensors, as follows:

Feature 2: *Shank sensors have higher all-time maximum of low-pass-filtered angular rates than thigh sensors.*

At this stage, we already classified each sensor as being related to a certain body segment, but we still need to determine on which leg each sensor is located. Without prior knowledge, we have no means to distinguish both legs in terms of *left* and *right*. Therefore, we let the two *foot* sensors represent one leg each. Consequently, we must find out which *shank* and *thigh* sensor belongs to which of the two *foot* sensors, in the following.

This goal is achieved by exploiting some fundamental characteristics of gait: In general, gait means that both legs alternate between stance and swing. During swing, both the

shank and the *foot* of the swinging leg rotate quickly. Let us approximate the swing phase of one leg by the period of time in which the angular rate of the *foot* sensor is higher than the all-time maximum angular rate of both *shank* sensors. We denote the duration of this time interval $T_{\approx swing}$.

Feature 3: *During swing phase of one leg, the shank sensor of that leg measures a higher low-pass-filtered angular rate than the other shank sensor.*

To evaluate this feature, we compare the integrals over $T_{\approx swing}$ for the angular rates of both *shank* sensors, as illustrated in Figure 2(a).

The final step toward the complete sensor-to-segment pairing is to pair a *thigh* sensor to its related *foot* sensor. For this purpose, the zero-mean jerk, i.e. the time derivative of the acceleration signal, was found to be a useful signal. Just like the angular rates for *foot* and *shank* sensors, the jerk of the *thigh* sensors alternates between high phases and low phases. These high-*thigh*-jerk phases appear a little later than (approximated) swing phases of the corresponding foot. We quantify this time-shift to be approximately 70% of the swing duration $T_{\approx swing}$.

Feature 4: *Near the end of the swing phase of one leg, the thigh sensor of that leg measures a higher low-pass-filtered zero-mean jerk than the other thigh sensor.*

The evaluation of this feature is illustrated in Figure 2(b). Note that the time shift of the integration interval is not absolute, but relative to $T_{\approx swing}$ and therefore, adaptive to different walking velocities.

Once we identified the body segment that each sensor is attached to, we can start the sensor-to-segment calibration for the *shank* and *thigh* sensors.

B. Sensor-to-Segment calibration

Recall that the orientations in which the sensors are attached to their segments are typically unknown. Thus, in order to calculate knee joint angles, we must first identify the knee joint axis coordinates in the local frames of the *thigh* and *shank* sensors [8]. It is important to note that these coordinates do not change in time, since the sensors are (almost) rigidly connected to the segments. As pointed out before, the axis coordinates are typically determined by means of precisely defined calibration movements, which

are difficult or impossible to perform for most patients with motion impairments. Therefore, we choose a different approach: We exploit the kinematic constraints of joints to achieve sensor-to-segment calibration from measurement data of arbitrary motions, as originally explained in [7].

The method that is presented here is an adaptation of a method that has previously been described for estimation of knee flexion and ankle dorsiflexion angles [8]. In that previous work, the sensor-to-segment calibration was found to be more influenced by relative motions between the skin that the sensor is attached to and the bones that confine the joint angle. These soft-tissue effects are typically large during toe-off and initial contact [8]. That makes it difficult to identify sensor-to-segment orientations from data that was recorded during walking. A careful analysis of recorded data led to the conclusion that the aforementioned relative motion is strongly related to the sensor rotating around the longitudinal axis of the segment. In the following, this finding is exploited to achieve sensor-to-segment calibration based on walking data.

Without loss of generality, consider only one leg from now on. We approximate the longitudinal axis of each segment by averaging the measured acceleration over one second during gait. We then implement a filter that rejects measurements from sample instants during which

- the Euclidean norms of the measured angular rates are below some small threshold or
- the *thigh* sensor was rotating primarily around the longitudinal axis of the *thigh* or
- the *shank* sensor was rotating primarily around the longitudinal axis of the *shank*,

where the last two criteria are evaluated by setting a threshold on the scalar product of the (normalized) current gyroscope reading and the approximated longitudinal axis of each segment.

The measured angular rates $\mathbf{g}_{\text{thigh}}(t) \in \mathbb{R}^3$ and $\mathbf{g}_{\text{shank}}(t) \in \mathbb{R}^3$ that pass this filter are stored in buffers $\mathbb{G}_{\text{shank}}$ and $\mathbb{G}_{\text{thigh}}$. As soon as the buffers $\mathbb{G}_{\text{shank}}$ and $\mathbb{G}_{\text{thigh}}$ each contain at least ten elements, we start a Gauß-Newton optimization procedure in order to find the unit-length axis coordinates $\mathbf{j}_{\text{thigh}} \in \mathbb{R}^3$ and $\mathbf{j}_{\text{shank}} \in \mathbb{R}^3$ that minimize (in a least squares sense) the left-hand side of the kinematic constraint of angular rates of hinge joints [7]

$$\|\mathbf{g}_{\text{shank}}(t) \times \mathbf{j}_{\text{shank}}\|_2 - \|\mathbf{g}_{\text{thigh}}(t) \times \mathbf{j}_{\text{thigh}}\|_2 = 0 \quad \forall t, \quad (1)$$

for all samples in $\mathbb{G}_{\text{shank}}$ and $\mathbb{G}_{\text{thigh}}$. After three Gauß-Newton steps, we obtain optimized axis coordinates, which then serve as starting points for the next optimization that is started as soon as more measurement samples have passed the aforementioned filter and were added to $\mathbb{G}_{\text{shank}}$ and $\mathbb{G}_{\text{thigh}}$. This procedure repeats until $\mathbb{G}_{\text{shank}}$ and $\mathbb{G}_{\text{thigh}}$ both contain at least 30 elements. At a sampling rate of $f_s = 50$ Hz, this is typically achieved after approximately three to five seconds of walking.

Note that the relatively small number of 30 samples in this optimization problem is a large benefit in terms of computational cost and allows realtime implementations even on computationally low-potent systems. Note furthermore that the method exploits a kinematic constraint that becomes manifest in any arbitrary motion of the joint [7], i.e. it does *not* depend on the user walking in a certain (physiological) manner or at a certain velocity.

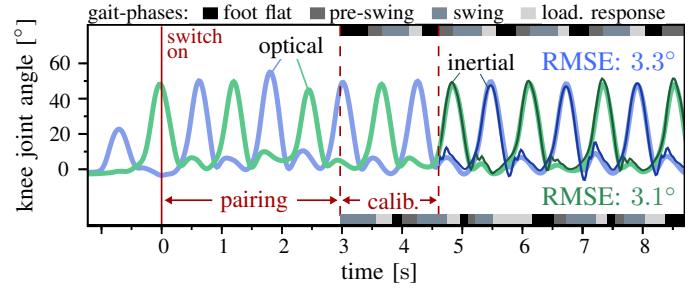


Figure 3: Sensor-to-segment pairing and calibration are completed in less than five seconds. After the calibration, knee joint angles are determined, which coincide well with measurements of an optical reference system.

Please note that the sensor-to-segment pairing has to be completed before the sensor-to-segment calibration can start, but in order to minimize the required time for the complete calibration procedure, the sensor-to-segment calibration uses also the data gathered during the sensor-to-segment pairing. Due to this, the entire sensor-to-segment pairing and calibration takes only about three to five seconds, as illustrated in Figure 3.

III. EXPERIMENTAL EVALUATION

In order to determine the reliability of the proposed sensor-to-segment pairing as well as calibration, we evaluated the data of three different experiments with several subjects and walking-trials. In all trials, the subjects were equipped with the proposed setup of six IMUs on the lower limbs. All subjects walked on a straight line at either slow, medium (self-selected) or fast pace.

We analyzed 85 walking-trials of five healthy subjects, 395 trials of eleven healthy barefoot walking subjects, who each walked at slow, normal and fast pace, and 53 trials of six ambulatory elderly patients suffering from Parkinson’s disease, who walked at self assessed speed and partially with walking frame. In the last experiment the attachment position of the right *thigh* sensor was varied between lateral, lateral low and frontal position. In addition, reference measurements for the knee joint angles were obtained from a marker-based optoelectronic motion capture system.

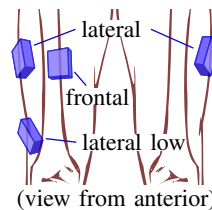
TABLE I: Success rate of the sensor-to-segment pairing

	16 subjects			6 patients
speed	slow	medium	fast	self assessed
trials	132	216	132	53
pairing	99.2%	100%	100%	100%

Table I presents the results of the sensor-to-segment pairings. Please note that only a correct classification of *all*

TABLE II: Influence of thigh sensor placement

sensor position	pairing success	knee angle accuracy
lateral	99.7%	$3.2^\circ \pm 1.7^\circ$
frontal	99.5%	$3.9^\circ \pm 2.2^\circ$
lateral low	100.0%	$3.0^\circ \pm 1.6^\circ$
average	99.7%	$3.4^\circ \pm 1.8^\circ$



six sensors was counted as a successful trial. A classification rate of 532 out of 533 trials is achieved for all subjects including fast and slow walkers as well as barefoot and shoe walkers and even Parkinson patients with walking frames.

In Table II we see the results of the sensor-to-segment pairing and the joint angle comparison for different thigh sensor positions. While the left thigh sensor is always attached to the *lateral* position, three positions (*lateral*, *lateral low* and *frontal*) are considered for the right thigh sensor. Even for the two asymmetric mountings, the classification rate remains very close to 100%.

To evaluate the reliability of the sensor-to-segment calibration, the knee-joint-axis coordinates with respect to each local sensor frame are estimated visually from sensor setup photos of each subject of the barefoot-walking trials. Although this method is certainly quite imprecise, the comparison of the photo-estimated axis coordinates to the results of the calibration method allows us to check for large deviations and unreasonable identification results. On average, this comparison yields disagreements of $18^\circ \pm 7^\circ$. Since the photo-based estimation procedure was found to have intra-rater and inter-rater reliabilities of about 15° , we conclude that the results of the automatic sensor-to-segment calibration are at least reasonable.

A more quantitative but also less direct approach toward evaluation of the sensor-to-segment calibration is to compare the knee joint angle measurements, which strongly rely on the calibration, to the measurements of the optical motion capture system. To this end, we calculate the root-mean-square deviations (RMSE) between inertial and optical knee angle measurements for each time interval during which a subject was walking through the limited observation volume of the optoelectronic system.

Table II shows RMSE values for three different thigh sensor positions. The average disagreement is approximately 3° . Similar accuracies were achieved by previously proposed but more restrictive methods (cf. [8] and references therein). This indicates that the sensor-to-segment calibration leads to state-of-the-art accuracies [8], although it uses only measurement data from walking rather than dedicated calibration motions.

IV. CONCLUSIONS

We proposed a set of methods that allow an IMU network to adjust to the user during gait in a plug-and-play manner. The experimental evaluation indicates that both the sensor-to-segment pairing and the sensor-to-segment calibration are highly reliable under a multitude of different conditions. The obtained joint angle accuracies of about 3° are comparable to the results that were reported in the literature for methods with more restrictive protocols including dedicated calibration movements. In order to obtain the most accurate results, the thigh sensor should be placed on the lateral side.

We conclude that the proposed methods enhance the practical usability of IMU-based gait analysis in many clinical applications. The user can independently attach the inertial sensors without the need for professional supervision, and precise realtime measurements are obtained without the need for restrictive calibration protocols. Since we refrained from using magnetometer readings, the methods are highly suitable for indoor environments. Our present and future work focuses on the development of plug-and-play neuro-prostheses that use the measurement signals of the user-adaptive inertial sensor network for feedback control.

ACKNOWLEDGMENTS

We would like to express our deep gratitude to Noelia Chia Bejarano and Simona Ferrante from Politecnico di Milano as well as to Gunnar Leivseth from NTNU Trondheim who provided some of the datasets that were analyzed in the experimental evaluation section.

REFERENCES

- [1] J.C. Moreno, A.J. del-Ama, A. de Los Reyes-Guzmán, Á. Gil-Agudo, R. Ceres, J.L. Pons, "Neurobotic and hybrid management of lower limb motor disorders: a review", *Medical & Biological Engineering & Computing*, 49(10):1119-30, 2011.
- [2] J.J. Daly, J. Zimbelman, K.L. Roenigk, J.P. McCabe, J.M. Rogers, K. Butler, R. Burdsall, J.P. Holcomb, E.B. Marsolais, R.L. Ruff, "Recovery of coordinated gait: randomized controlled stroke trial of functional electrical stimulation (FES) versus no FES, with weight-supported treadmill and over-ground training", *Neurorehabil Neural Repair*, 25(7):588-96, 2011.
- [3] T. Seel, M. Valtin, C. Werner, T. Schauer, "Multivariable Control of Foot Motion During Gait by Peroneal Nerve Stimulation via two Skin Electrodes", *IFAC-PapersOnLine*, 48(20):315-320, 2015.
- [4] J. Favre, B.M. Jolles, R. Aissaoui, K. Aminian, "Ambulatory measurement of 3D knee joint angle", *Journal of Biomechanics*, 41, pp. 1029-1035, 2008.
- [5] K.J. O'Donovan, R. Kamnik, D.T. O'Keefe, G.M. Lyons, "An inertial and magnetic sensor based technique for joint angle measurement", *Journal of Biomechanics*, 40, pp. 2604-2611, 2007.
- [6] A. Cereatti, D. Trojaniello, U.D. Croce, "Accurately measuring human movement using magneto-inertial sensors: techniques and challenges", *2015 IEEE International Symposium on Inertial Sensors and Systems (ISISS)*, pp. 1-4, 2015.
- [7] T. Seel, T. Schauer, J. Raisch, "Joint axis and position estimation from inertial measurement data by exploiting kinematic constraints", *Proceedings of the IEEE International Conference on Control Applications*, pp. 45-49, 2012.
- [8] T. Seel, T. Schauer, J. Raisch, "IMU-Based Joint Angle Measurement for Gait Analysis", *Sensors*, 14 (4):6891-6909, 2014.
- [9] D. Weenk, B. van Beijnum, C. Baten, H. Hermens, P. Veltink, "Automatic identification of inertial sensor placement on human body segments during walking", *Journal of NeuroEngineering and Rehabilitation*, 10:31, 2013.
- [10] S. Lambrecht, J.P. Romero, J. Benito-Leon, E. Rocon, J.L. Pons, "Task independent identification of sensor location on upper limb from orientation data", *Engineering in Medicine and Biology Society, 36th Annual International Conference of the IEEE*, pp. 6627-6630, 2014.
- [11] K. Kunze, P. Lukowicz, H. Junker, G. Trster, "Where am I: Recognizing on-Body positions of wearable sensors", *Location- and Context-Awareness, Volume 3479 of Lecture Notes in Computer Science*, Springer, 2005:264-275.
- [12] A. Mannini, A.M. Sabatini, S.S. Intille, "Accelerometry-based recognition of the placement site of a wearable sensor", *Pervasive and Mobile Computing*, vol. 21, pp. 62-74, 2015.
- [13] T. Seel, L. Landgraf, Vctor Cermeo Escobar, J. Raisch, T. Schauer, "Online Gait Phase Detection with Automatic Adaption to Gait Velocity Changes Using Accelerometers and Gyroscopes", *Biomedical Engineering / Biomedizinische Technik*, vol. 59, pp. 795-798, 2014.
- [14] T. Seel, D. Graurock, T. Schauer, "Realtime Assessment of Foot Orientation by Accelerometer and Gyroscopes", *Current Directions in Biomedical Engineering*, 1 (1):466-469, 2015.
- [15] N. Chia Bejarano, E. Ambrosini, A. Pedrocchi, G. Ferrigno, M. Monticone, S. Ferrante, "A Novel Adaptive, Real-Time Algorithm to Detect Gait Events From Wearable Sensors", *IEEE Transactions on Neural Systems and Rehabilitation Engineering*, 23(3):413-422, 2015. doi: 10.1109/TNSRE.2014.2337914